

HIGH SPEED STEEL TOOL WEAR AFTER WOOD MILLING IN THE PRESENCE OF HIGH TEMPERATURE TRIBOCHEMICAL REACTIONS

B. Porankiewicz,^{a*} P. Iskra,^b K. Józwiak,^c C. Tanaka,^d and W. Zborowski^e

Wear patterns were analyzed for High Speed Steel (HSS) SKH51 cutting tools after milling wood of four wood species having very different High Temperature Tribochemical Reactions (HTTR), wood density and very low hard mineral contamination (HMC). The experimental results showed that the HTTR can be an important factor influencing acceleration of cutting tool wear.

Keywords: Cutting edge recession; High speed steel; Wood, milling; High temperature tribochemical reactions

Contact information: a: Emeritus Dr Hab; b: Wood Research Center (CRB) Pavilion Gene H. Kruger, Laval University, Quebec G1K 7P4, QC, Canada; c: Poznań University of Technology, pl. Marii Skłodowskiej-Curie 5, 60 965 Poznań, Poland; d: Emeritus, PhD, Professor; e: Poznań University of Economics, al. Niepodległości 10, 60967 Poznań, Poland; *Corresponding author: poranek@amu.edu.pl

INTRODUCTION

Recent work has shown evidence that unusually fast dulling of cutting tools after machining specific wood specimens was associated with large mineral contamination, which explains earlier reports (Amos 1952). Such effects may be accompanied by high-temperature tribochemical reactions (HTTR) (Porankiewicz 2003 a, b). However, there have been no published examples of fast cutting tool wear related to wood species that do not accumulate silica (Amos 1952). There has been a need to examine such effects by use of suitable machining experiments.

In the present work the HSS tool cutting edge recessions were studied during longitudinal milling of four wood species. The specimens were especially chosen for very low hard mineral contamination, having a very wide range of high and low HTTR relative to the material of a cutting tool.

EXPERIMENTAL

Machining experiments were performed in the laboratory of Matsue University, Japan, using a Shoda Fanuc NC-3 computer numerical controlled machine. The milling was performed under following machining conditions:

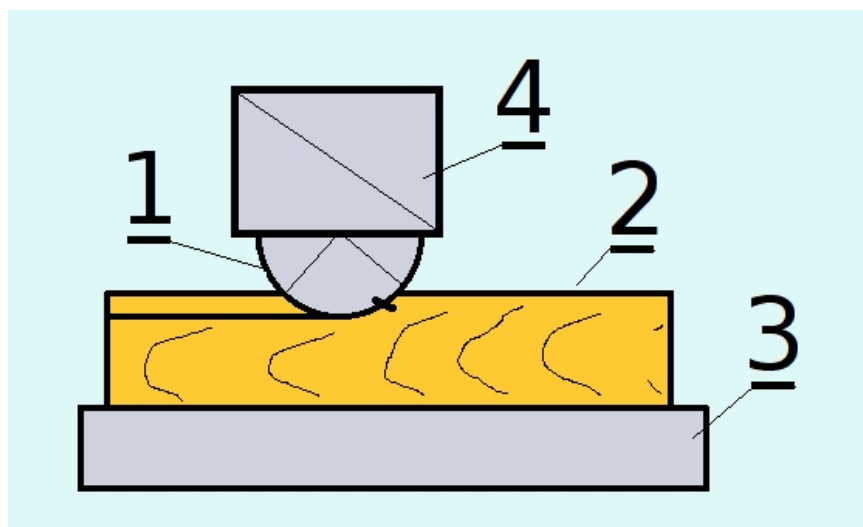


Fig. 1. Scheme of the cutting situation; 1 - cutting tool, 2 - working piece, 3 - machine table, 4 - electrical motor

- Material of the cutting edge SKH51, according to JIS: (W 5.5 - 6.7 %; Mo 4.5 - 5.5 %; V 1.6 - 2.2 %; Cr 3.8 - 4.5 %; C 0.8 - 0.88 %).
- Hardness of the cutting edge material 64 HRC.
- Rotational speed of a spindle $n = 2864 \text{ min}^{-1}$.
- Cutting speed $v_C = 30 \text{ m/s}$.
- Number of cutting edges $z = 1$.
- Feed rate per tooth $f_Z = 0.1 \text{ mm}$.
- Rake angle $\gamma_F = 30^\circ$.
- Sharpness angle $\beta_F = 55^\circ$.
- Cutting depth $g_S = 1.5 \text{ mm}$.
- Moisture content $m_C = 11 \%$.

The main properties of four wood specimens are shown in Table 1. For estimation of the HTTR of products of thermal degradation of wood towards iron, a method based on a Thermal Gravimetric Analysis (TGA), described in earlier works (Porankiewicz 1998, 2000) was employed. A fine broken iron powder, representing the binder in steel tool material, having weak magnetic reaction, was applied for thermal analysis, according to the method developed. In an environment involving an unbalanced pulse magnetic field (50 Hz, $2.5 \cdot 10^{-4} \text{ N/(A}\cdot\text{m)}$) of a Shimadzu TGA-50 apparatus heating coil, a remarkable acceleration (to detectable level) of the HTC effect of products of wood thermal degradation on the Fe particles takes place (Porankiewicz 2003a, b). The TGA tests were performed in free ambient air flow, up to 750°C , by a temperature elevation rate of 50°C/min , in porcelain crucibles. For mixed analyses the Fe and wood powder were used in the proportion of 17 mg and 3 mg. The Fe particles were approximately of $2.5 \mu\text{m}$ in diameter, according to the Functional Spectral Signature (FSS) method. A rapid mass increase on the dTG plots, a first derivative of mass m against time t (dm/dt), were associated with peaks of the HTTR. For characterization of the HTTR of products

of thermal decomposition of wood and iron, a binder of the cutting edge material, a R_{MW} quantifier, calculated from formula (1), was applied.

Table 1. Wood Specimens Used in the Experiment

Wood spec. no.	Name	Name	Country of origin	Wood density (kg/m ³)	Photograph
1	Yellow meranti	<i>Shorea faguettiana</i> F.	Indonesia	626	
2	Douglas fir	<i>Japanese Douglas Fir</i>	Japan	522	
3	Kempas	<i>Koompassia malaccensis</i> M.& B.	Indonesia	880	
4	Keyaki	<i>Zelkova serrata</i>	Japan	706	

$$R_{MW} = \frac{\sum (R \cdot T \cdot T_z)}{m \cdot \sum R \cdot \sum T \cdot \sum T_z} \quad (1)$$

New terms in equation (1) are:

- R - Height of a single corrosion peak (mg/min⁻¹),
- ΣR - Summation height of a single corrosion peak (mg/min⁻¹),
- T - Temperature of a single corrosion peak maximum (°C),
- ΣT - Summation of a single corrosion peak maximum (°C),
- T_z - Temperature range of single corrosion peak (°C),
- ΣT_z - Summation of temperature ranges T_z (°C),
- m - Mass of iron specimen (mg).

The R_{MW} quantifier, according to formula (1), appears as a weighted (according to width and height of HTTR peak) average speed of the iron specimen mass increase in corrosion peaks, up to 540°C, assumed as the maximum temperature of the cutting edge during milling. More complex HTTR peaks observed in the present work, consisting of large (wide and high) and small (narrow and short) elements, was one reason for using special methods of analysis (shown in Fig. 2). This approach is different from what has been used in experiments that have been carried out heretofore.

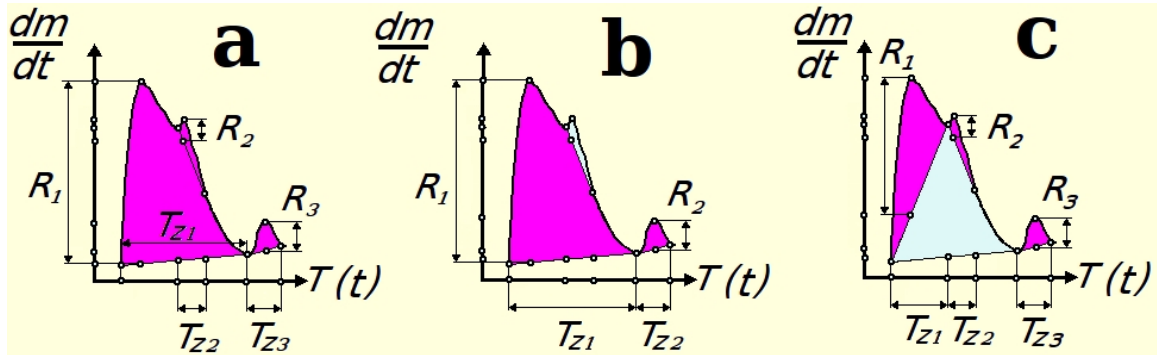


Fig. 2. Parameters of HTTR peaks, according to: a - method I, b - method II and c - method III; R - height of corrosion peak, T - temperature, Tz - temperature range of corrosion peak, t - time

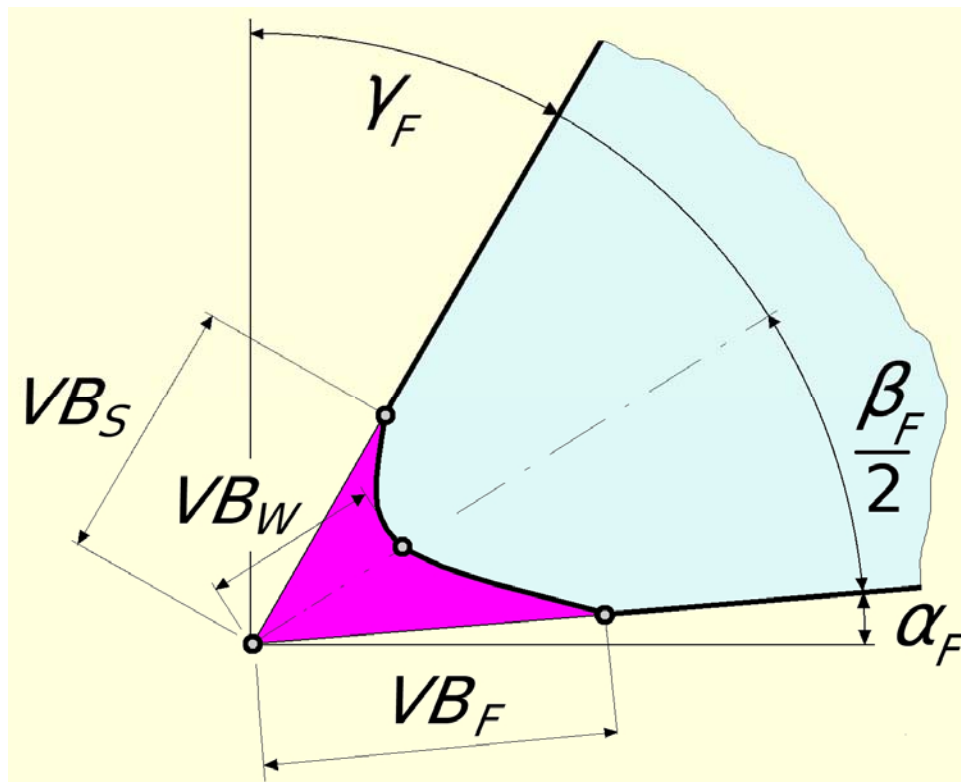


Fig. 3. Parameters describing a worn cutting edge

The cutting edge recession was measured on the clearance surface VB_F , the rake (face) surface VB_S , and in the direction of the bisector of the wedge angle clearance surface VB_W (Fig. 3). The cutting edge profiles were scanned, under vertical magnification of $\times 50$, with the use of a stylus, perpendicular to the edge in three places separated by 1 mm.

For evaluation of the content of the HMC of the wood specimens analyzed, a combustion method, expanded by additional burning of the glass filter, was applied

(Porankiewicz et al. 2003, 2005, 2006). Wood specimens were analyzed using a Scanning Electron Microscope (SEM) and Electron Dissipative Spectrum (EDS) in regards to silica-like structures. The specimens were sputtered by carbon before SEM analysis.

In the evaluation process of statistical dependencies $VB_F = f(L_C)$, $VB_W = f(L_C)$, and $VB_S = f(L_C)$ for all examined wooden specimens, a linear function, a second order multinomial formula, as well as a power type and a exponential function, were analyzed in preliminary calculations. The most adequate model, according to the above assumptions, appeared to be equation (2). Estimators for formula (2) were evaluated from an experimental matrix containing 5 measuring points.

$$VB_F = a_1 \cdot L_C^{a_2} + a_3 \quad (\mu\text{m}) \quad (2)$$

The cutting path L_C , in formula (2) was expressed in (m). During the evaluation process, elimination of un-important or low-import estimators was done by use of coefficient of relatively importance C_{RI} , defined by formula (3), by the assumption $C_{RI} > 0.1$.

$$C_{RI} = \frac{(SK - SK_{OK})}{SK} \cdot 100 \quad (\%) \quad (3)$$

In formula (3) the new terms are:

- SK_{OK} - Summation of square of residuals, by $c_K = 0$.
- c_K - K estimator number in statistical model evaluated.

The summation of residuals square SK , standard deviation SD , and the square of correlation coefficient of the predicted and observed values R^2 were used for characterization of approximation quality. Calculations were performed at Poznań Networking & Supercomputing Center PCSS, on a SGI Altix 3700 computer, using a special optimization program, based on a least squares method combined with gradient and Monte Carlo methods (Porankiewicz 1988) with further changes.

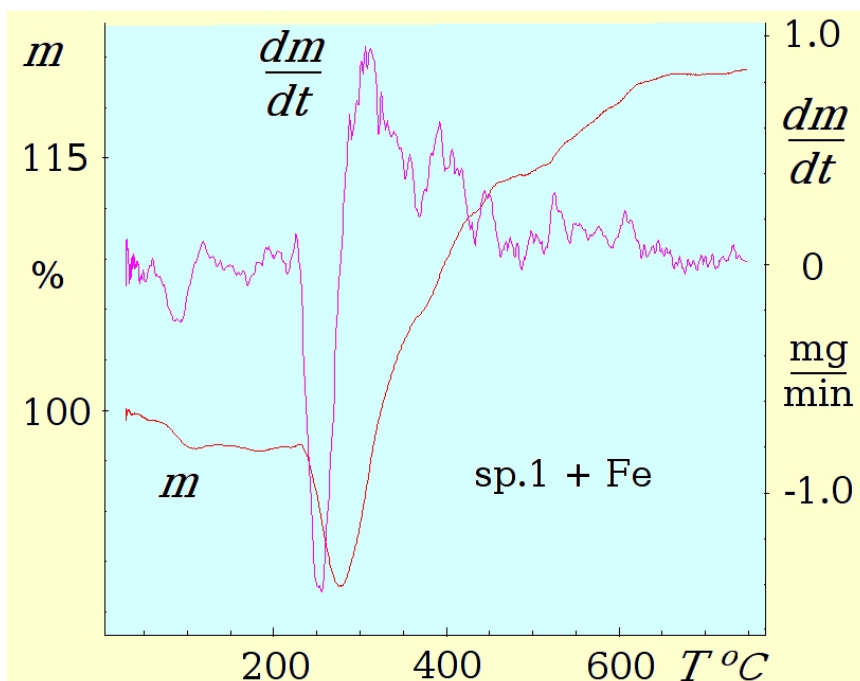
RESULTS AND DISCUSSION

Table 2 summarizes the R_{MW} quantifiers and the content C_{MC} as well as the size S_{MC} of HMC in fraction $f_7 < 0.05$ mm in the wood specimens analyzed. From Table 2 it can be seen that the R_{MW} quantifiers for specimen no. 4 were the largest of all, many times larger than values for the others specimens. The reason is that the HTTR peak visible in Fig. 7 is the largest of all, and, accompanied by only a few small and narrow corrosion peaks. A large amount of small and narrow corrosion peaks (which can be seen in Figs. 4, 5, and 6) was a reason for decreasing values of the R_{MW} quantifiers for wood specimens 1, 2, and 3. The largest HSS cutting edge recessions for specimen no. 4 (Table 3) might be associated with the highest HTTR (Table 2) between iron, binder in the HSS tool material, and products of thermal degradation of components of wood.

Table 2. The HTTR Quantifier $R_{MW} \cdot 10^{-3}$, Content C_{MC} and Size S_{MC} of Fraction 7 of the Hard Mineral Contamination C_{MC} of Wood Specimens Analyzed

No.	Method I (mg^{-1})	Method II (mg^{-1})	Method III (mg^{-1})	C_{MC} (mg/kg)	S_{MC} (μm)
1	0.106	0.416	0.086	7	14.6
2	0.086	0.227	0.093	100	8.1
3	0.153	0.408	0.114	10	19.6
4	2.05	9.281	2.797	38	19.5

All wood specimens were recognized as very low hard mineral contaminated. Very low HMC, together with rather large HTTR, expressed by the R_{MW} quantifier was the first case evidenced during HSS tool wearing experiments (Porankiewicz et al. 2005, 2006). Particles of HMC extracted from wood specimens tested are shown in Fig. 8. In all wood specimens, regular, ball-like, and irregular particles were observed. The size of most particles was lower than $10 \mu\text{m}$, but every wood specimen also contained several larger particles, as high as from 20 to $70 \mu\text{m}$. The ball-like particles, which were supposed to be a micro meteorites, were evidenced in earlier work (Porankiewicz et al. 2005). The surface of several particles extracted from wood specimen no. 4, of *Zelkova serrata* (Fig. 8) seems to be coated, and partially fractured, by a glaze, which could not be seen on particles from other wood specimens. Several small aggregates of HMC particles were also found out in wood specimen no. 4 (Fig. 8). This was similar to the wood described by Keirung (*Combretocarpus sp.*) and Oil Palm (*Elais guineensis*) examined in earlier works (Porankiewicz et al. 2005, 2006).

**Fig. 4.** TGA (TG and dTG) plots of Fe together with the wood specimens no. 1, of the *Shorea faguetiana F.*

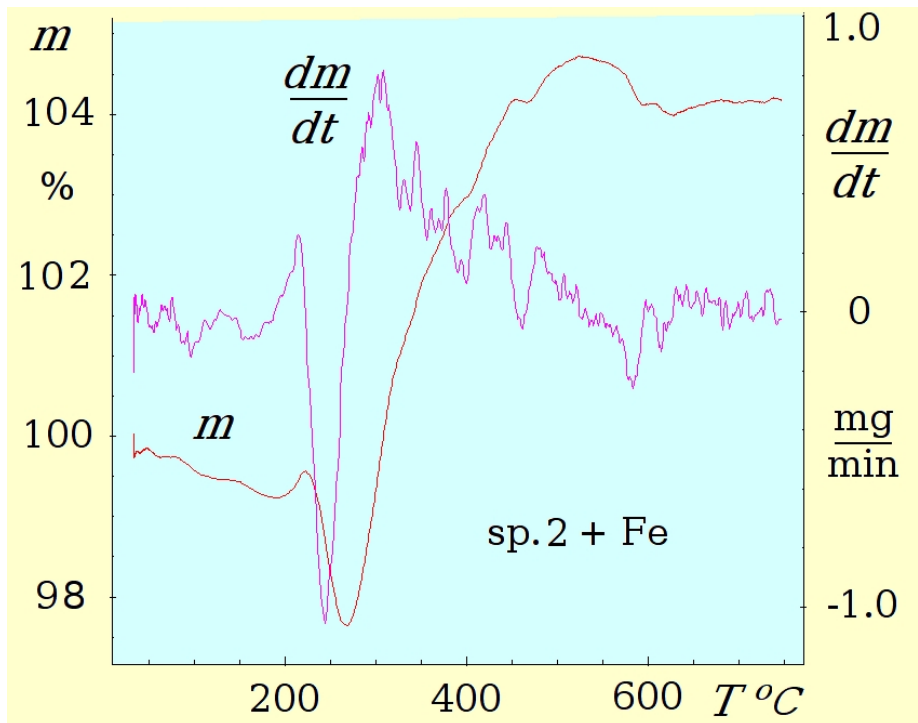


Fig. 5. TGA (TG and dTG) plots of Fe together with the wood specimen no. 2, of the *Japanese Douglas Fir*

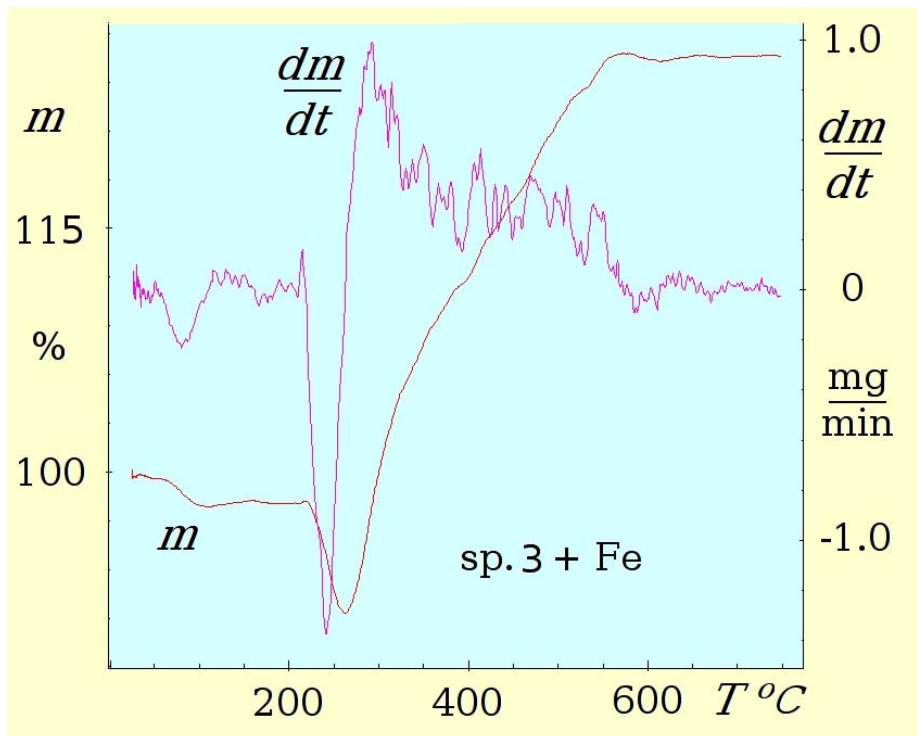


Fig. 6. TGA (TG and dTG) plots of Fe together with the wood specimen no. 3, of the *Koopassia malaccensis M.&B.*

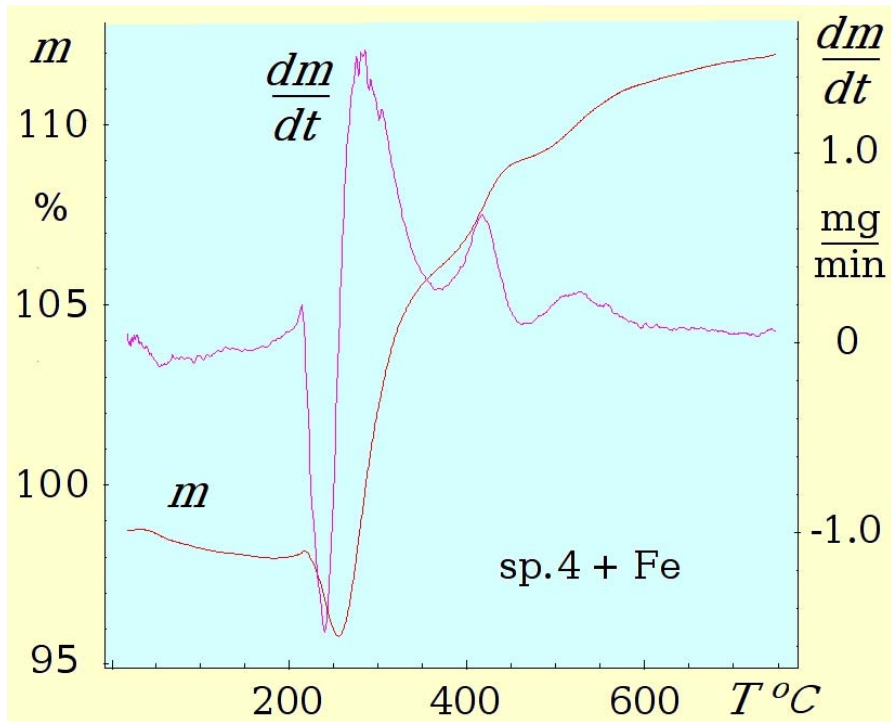


Fig. 7. TGA (TG and dTG) plots of Fe together with the wood specimen no. 4, of the *Zelkova serrata*

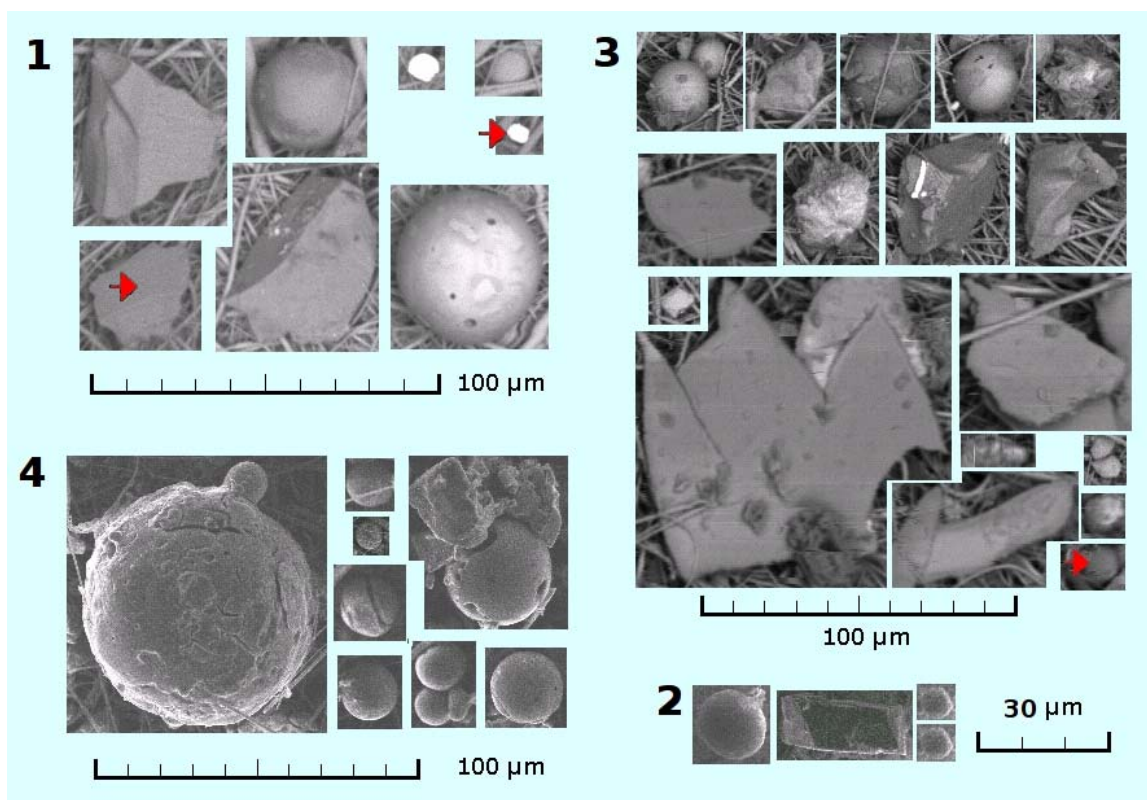


Fig. 8. SEM micrograph of hard mineral contamination extracted from the wood specimens

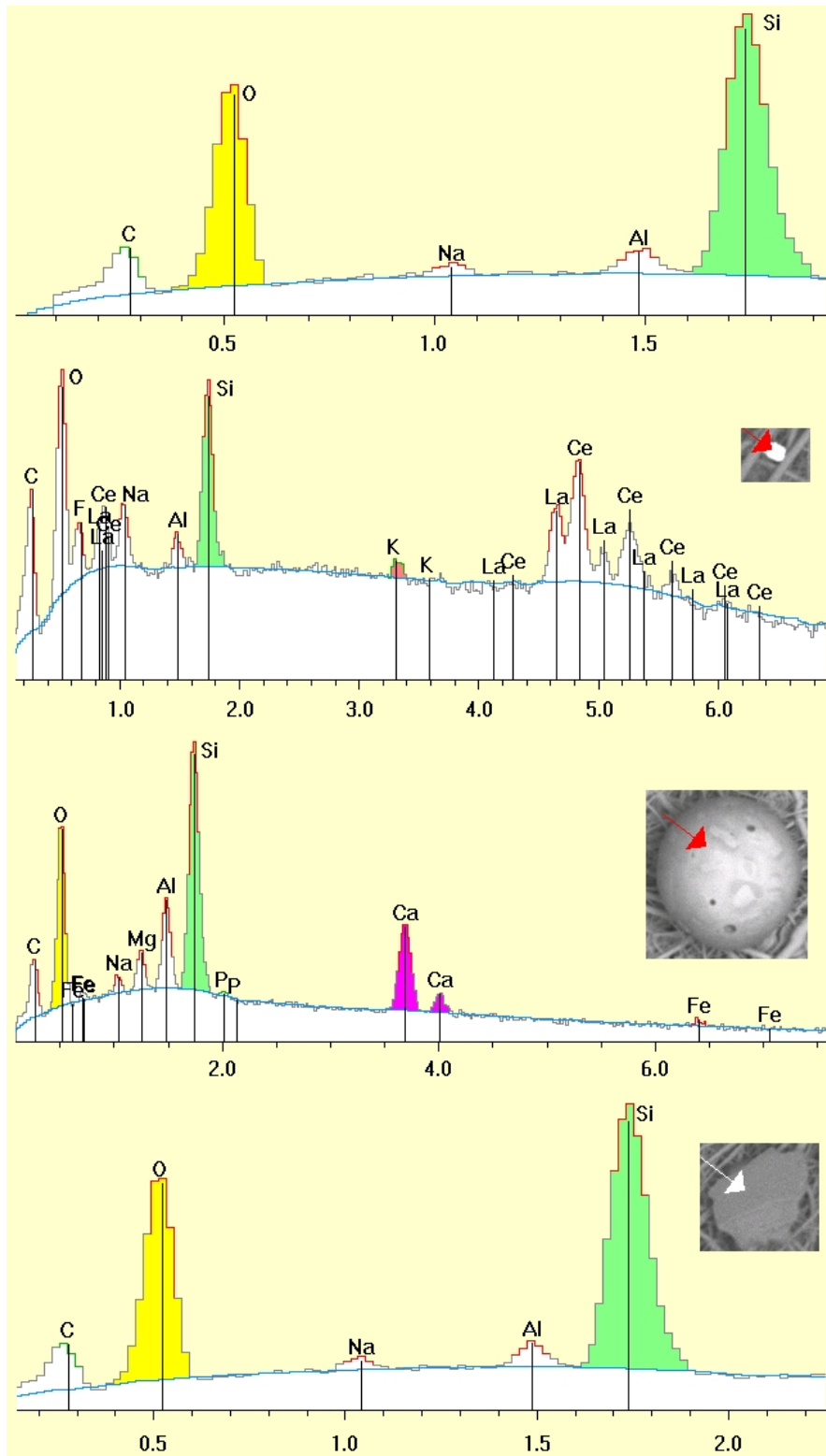


Fig. 9. EDS spectra for hard mineral contamination particle extracted from wood specimen no. 1, of the *Shorea faguetiana* F.

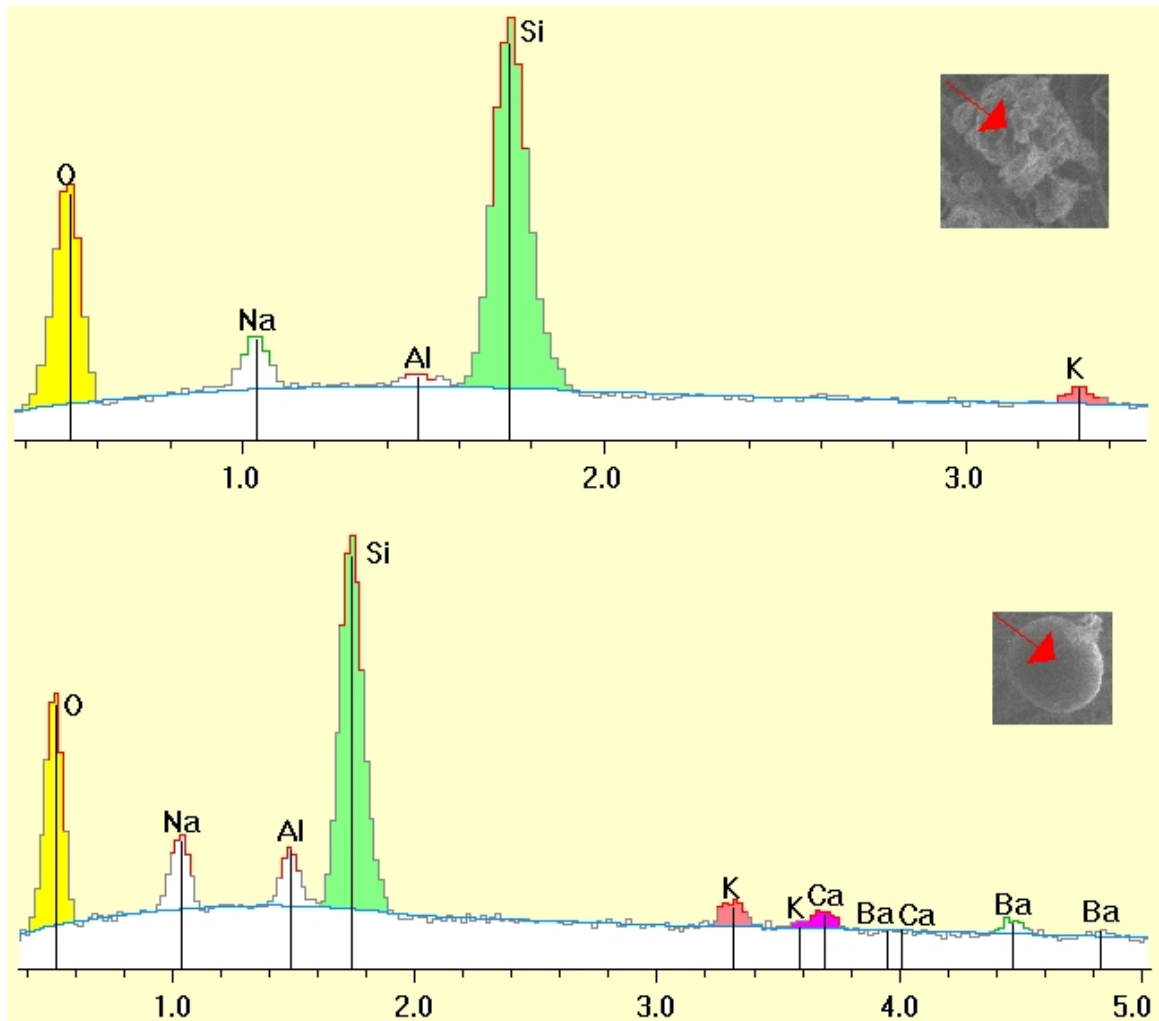


Fig. 10. EDS spectra for hard mineral contamination particle extracted from wood specimen no. 2, of the *Japanese Douglas Fir*

A significant amount of potassium (K), together with a certain amount of calcium (Ca) in ash, decreasing its melting temperature, was recognized as a reason for the creation of aggregates of HMC particles, as well as their glaze coating, during the burning procedure. The aggregates of HMC particles did not originate from the wood itself. The EDS examination (Figs. 9 through 12), performed for particles marked in red in Fig. 8, show that HMC particles present in the wood specimens analyzed, mainly consisted of silica (SiO_2), with very small admixture of Ca, K, sodium (Na), magnesium (Mg), and aluminum (Al), as well as barium (Ba), chromium (Cr), iron (Fe), cesium (Ce) and lanthanum (La) in the oxidized phase.

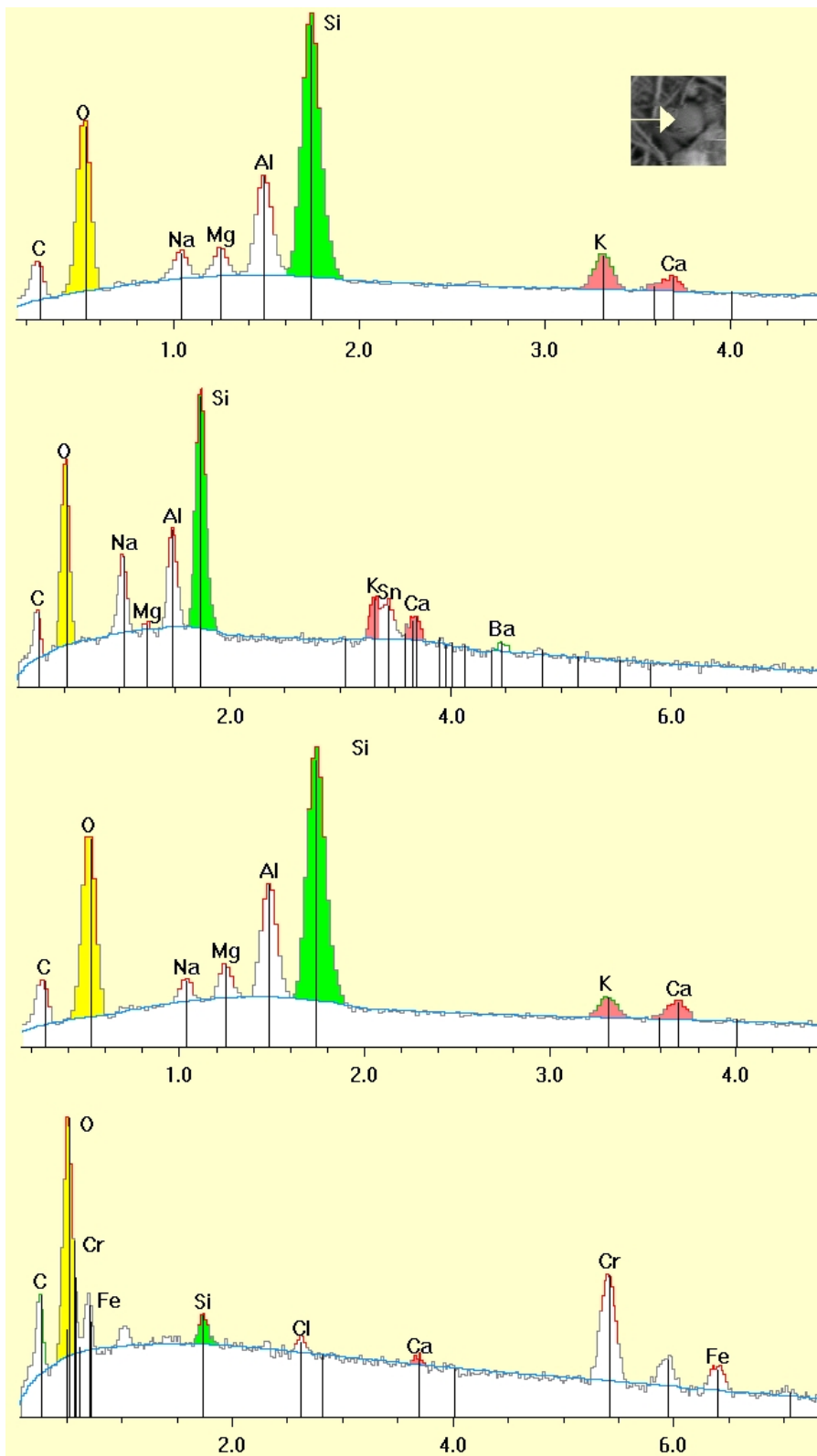


Fig. 11. EDS spectra for hard mineral contamination particles extracted from the wood specimen no. 3, of *Koombassia malaccensis* M.&B.

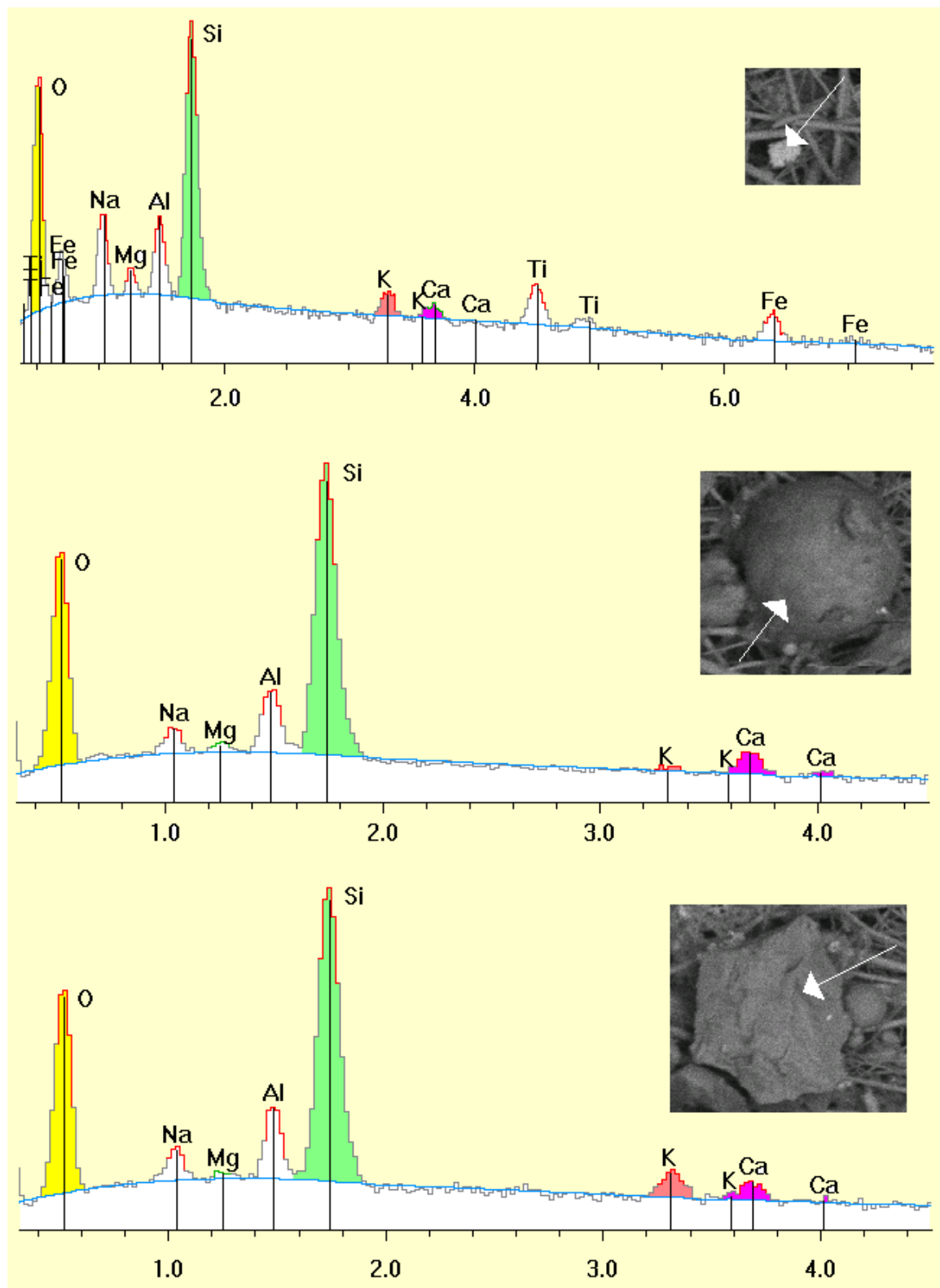
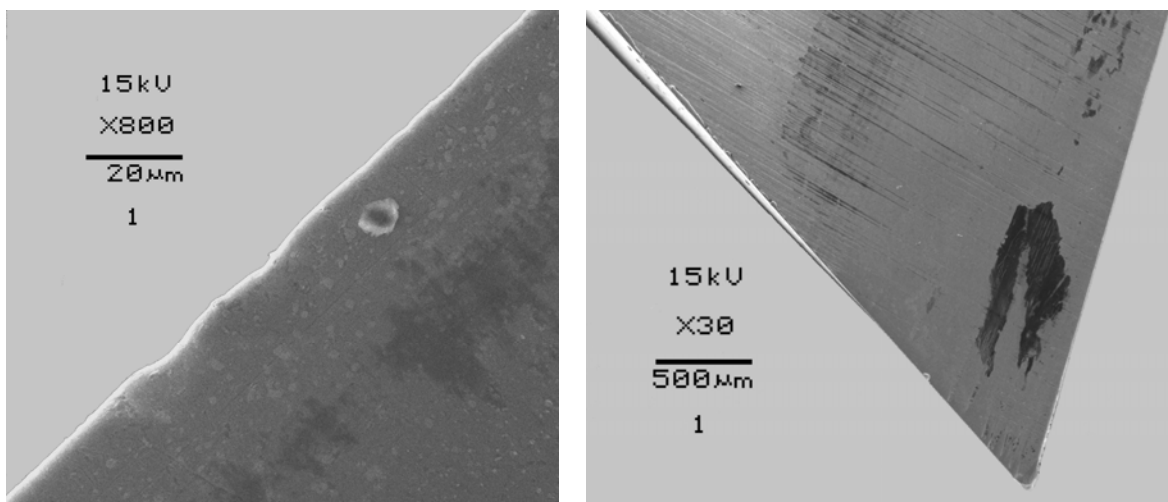


Fig. 12. EDS spectra for hard mineral contamination particles extracted from the wood specimen no. 4, of *Zelkova serrata*

Table 3. The Cutting Edge Recession VB_F , VB_W and VB_S for Analyzed Wood Specimens nrs. 1, 2, 3, and 4

No.	L_C (m)	VB_F	VB_W	VB_S
		(μm)		
1	0	37.7	22.4	30
	5000	6	10.5	7.5
	10000	9	10.5	7.5
	15000	9	10.5	7.5
	20000	9	11	8
2	0	35.2	19.9	26.2
	5000	35	17	16.5
	10000	39	18.5	17
	15000	41	19	17.5
	20000	41.5	19	17.5
3	0	38.4	18.7	27
	5000	10	14.5	13.5
	10000	13	15	16
	15000	14	17.5	26
	20000	16.5	17.5	26
4	0	60.5	45.9	55.7
	5000	134.5	34.5	34
	10000	190	51	41
	15000	195.5	72	63.5
	20000	232.5	78	84.5

**Fig. 13.** SEM image of the tool no. 1, after cutting wood of *Shorea faguetiana* F., by cutting path $L_C = 20000$ m

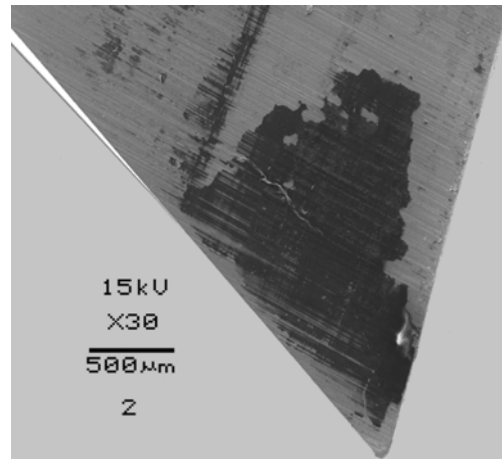
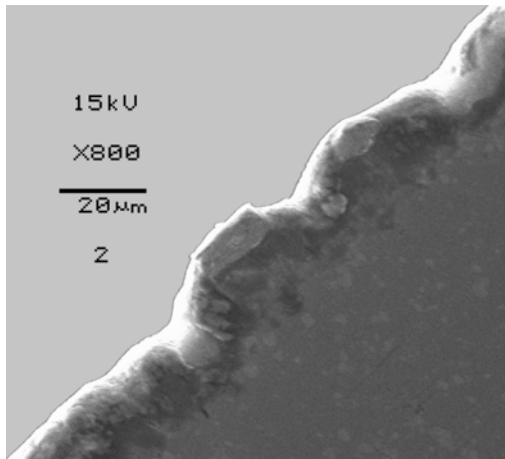


Fig. 14. SEM image of the tool no. 2, after cutting wood of *Japanese Douglas Fir*, by cutting path $L_C = 20000$ m

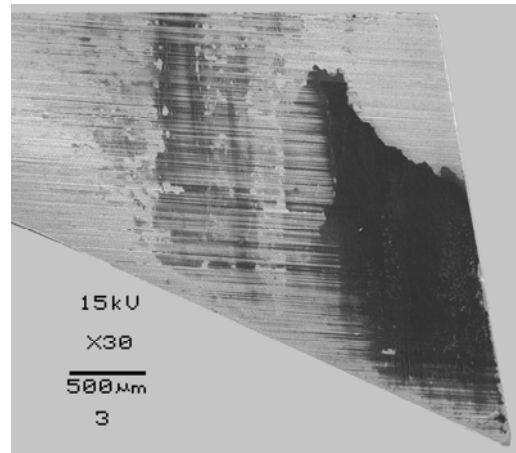
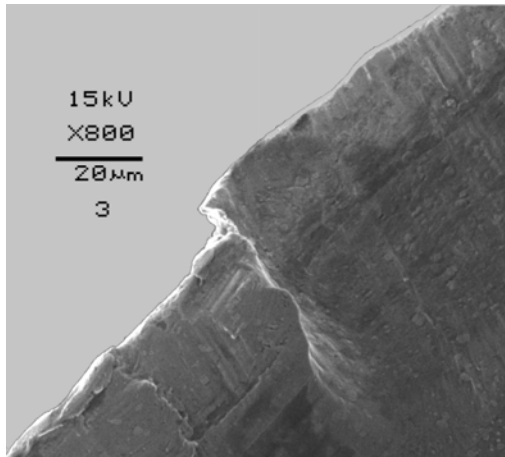


Fig. 15. SEM image of the tool no. 3, after cutting wood of *Koompassia malaccensis M.&B.*, by cutting path $L_C = 20000$ m

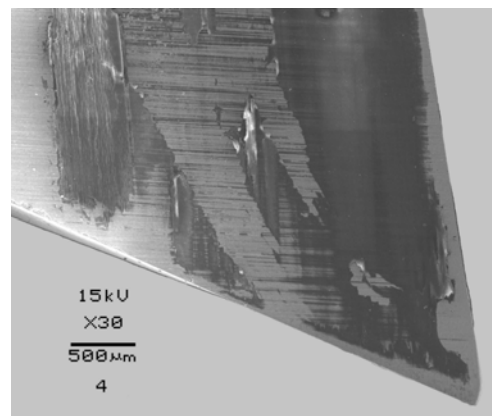
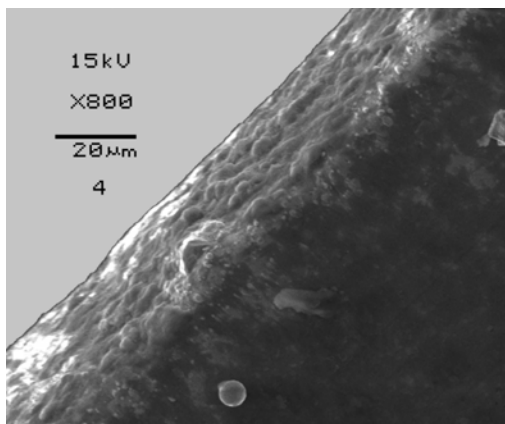


Fig. 16. SEM image of the tool no. 4, after cutting wood of *Zelkova serrata*, by cutting path $L_C = 20000$ m

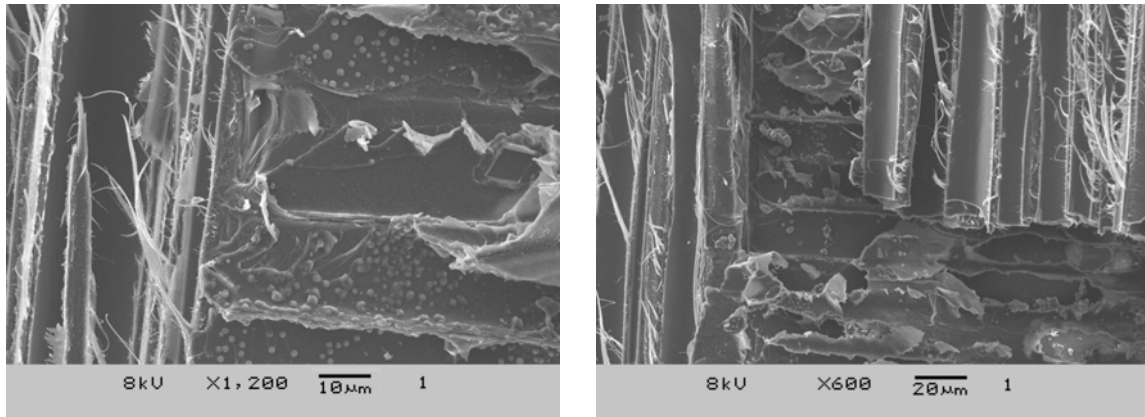


Fig. 17. SEM images of the Yellow meranti (*Shorea faguettiana* F.) wood specimen

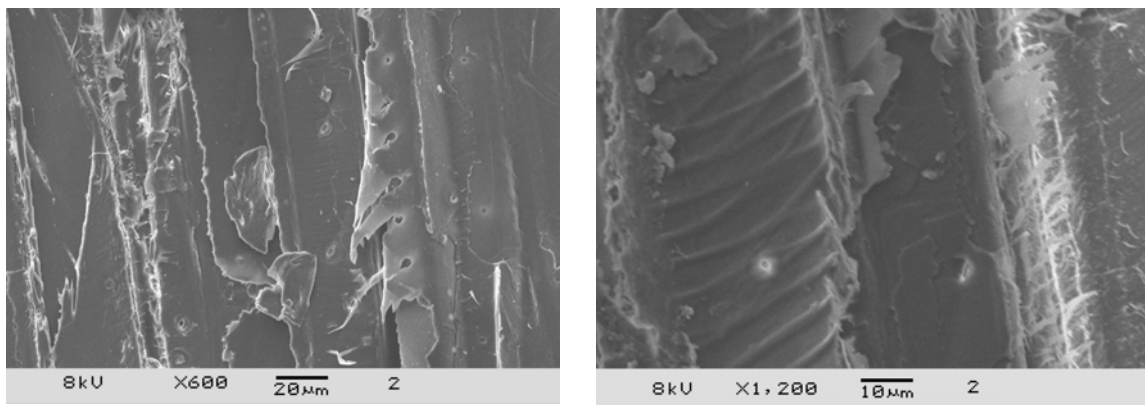


Fig. 18. SEM images of the Douglas fir (*Japanese Douglas Fir*) wood specimen

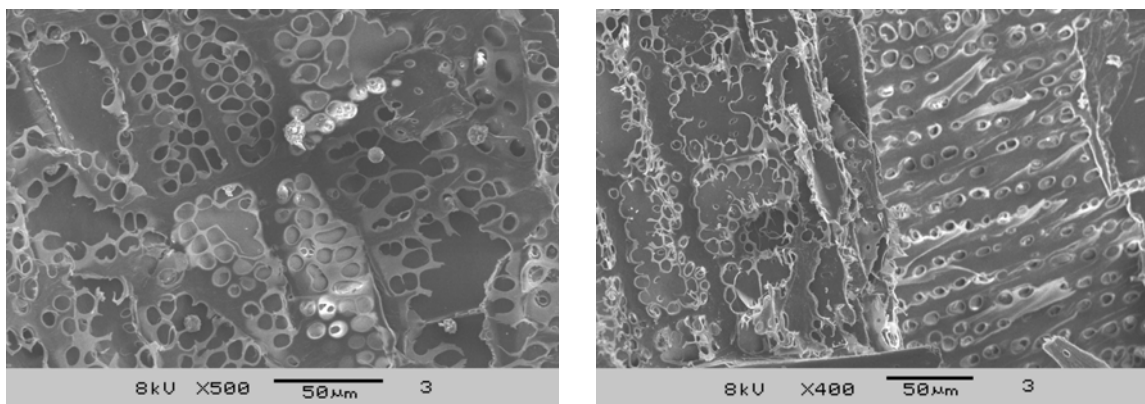


Fig. 19. SEM images of the Kempas (*Koompassia malaccensis* M.&B.) wood specimen

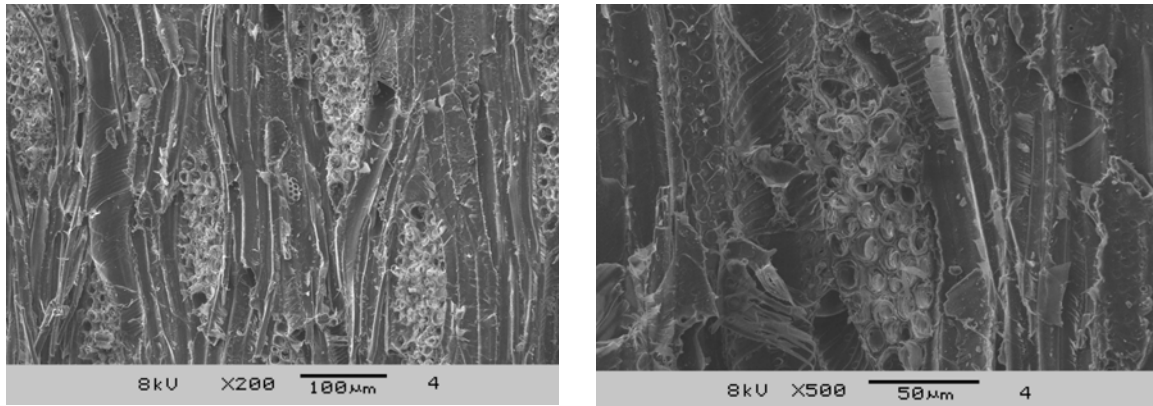


Fig. 20. SEM images of the Keyaki (*Zelkova serrata*) wood specimen

The large value of a square of correlation coefficient R^2 obtained for formulas (4) - (15) suggests that a power type function described the relationship well between the cutting edge recessions and the cutting path L_C , collected in the Table 3.

$$VB_F = 0.73624 \cdot L_C^{0.25885} + 57.68167 \quad (\mu\text{m}) \quad (4)$$

The approximation quality of the fit of the formula (4) for the *Shorea faguettiana* F., can be characterized by quantifiers: $SK=1.8$, $SD=0.8$, $R^2=0.97$.

$$VB_F = 12.2301 \cdot L_C^{0.12486} + 35.12797 \quad (\mu\text{m}) \quad (5)$$

The approximation quality of the fit of the formula (5) for the *Japanese Douglas Fir*, can be characterized by quantifiers: $SK=0.8$, $SD=0.5$, $R^2=0.99$.

$$VB_F = 0.52022 \cdot L_C^{0.34694} + 38.40476 \quad (\mu\text{m}) \quad (6)$$

The approximation quality of the fit of the formula (6) for the *Koompassia malaccensis* M.&B., can be characterized by quantifiers: $SK=0.6$, $SD=0.4$, $R^2=0.99$.

$$VB_F = 6.20298 \cdot L_C^{0.36458} + 60.37284 \quad (\mu\text{m}) \quad (7)$$

The approximation quality of the fit of the formula (7) for the *Zelkova serrata*, can be characterized by quantifiers: $SK=290.9$, $SD=9.8$, $R^2=0.99$.

$$VB_W = 21.614 \cdot L_C^{0.011488} + 8.9708 \quad (\mu\text{m}) \quad (8)$$

The approximation quality of the fit of the formula (8) for the *Shorea faguettiana* F., can be characterized by quantifiers: $SK=0.1$, $SD=0.2$, $R^2=0.998$.

$$VB_w = 8.7827 \cdot L_C^{0.08096} + 19.59289 \quad (\mu\text{m}) \quad (9)$$

The approximation quality of the fit of the formula (9) for *Japanese Douglas Fir*, can be characterized by quantifiers: $SK=0.2$, $SD=0.3$, $R^2=0.999$.

$$VB_w = 3.77433 \cdot L_C^{0.15562} + 18.69623 \quad (\mu\text{m}) \quad (10)$$

The approximation quality of the fit of the formula (10) for *Koompassia malaccensis M.&B.*, can be characterized by quantifiers: $SK=1.2$, $SD=0.6$, $R^2=0.99$.

$$VB_w = 0.20898 \cdot L_C^{0.60114} + 45.76476 \quad (\mu\text{m}) \quad (11)$$

The approximation quality of the fit of the formula (11) for the *Zelkova serrata* can be characterized by quantifiers: $SK=32.9$, $SD=3.3$, $R^2=0.99$.

$$VB_s = 7.569591 \cdot L_C^{0.02891} + 27.60787 \quad (\mu\text{m}) \quad (12)$$

The approximation quality of the fit of the formula (12) for the *Shorea faguetiana F.* can be characterized by quantifiers: $SK=0.1$, $SD=0.2$, $R^2=0.998$.

$$VB_s = 13.68515 \cdot L_C^{0.039547} + 23.542937 \quad (\mu\text{m}) \quad (13)$$

The approximation quality of the fit of the formula (13) for the *Japanese Douglas Fir*, can be characterized by quantifiers: $SK=0.03$, $SD=0.1$, $R^2=0.999$.

$$VB_s = 0.12184 \cdot L_C^{0.54549} + 24.02649 \quad (\mu\text{m}) \quad (14)$$

The approximation quality of the fit of the formula (14) for the *Koompassia malaccensis M&B.* can be characterized by quantifiers: $SK=16.4$, $SD=2.2$, $R^2=0.96$.

$$VB_s = 0.02844 \cdot L_C^{0.802514} + 56.94507 \quad (\mu\text{m}) \quad (15)$$

The approximation quality of the fit of the formula (15) for the *Zelkova serrata*, can be characterized by quantifiers: $SK=92.4$, $SD=5.5$, $R^2=0.98$.

The clearance surface of worn tool no. 1, shown in Fig 13, appeared to be well polished, with little cutting edge recession. Small, rounded areas of damage, visible on the cutting edge, probably occurred in an early stage of the cutting test. The HTTR probably did not contribute much to the total tool wearing process. The clearance surface of worn tool no. 2, shown in Fig 14, was also well polished with small cutting edge recession. However several instances of rounded damage occurred probably in the early stage of cutting test, suggesting the presence in the wood specimens of a medium-sized particles of hard mineral contamination. These particles were not detected in the ashing

procedure. In this case, the HTTR have probably have a very small contribution in the total cutting edge wearing process. The clearance surface of worn tool no. 3, shown in Fig. 15 has a single instance of visible, not rounded damage, while there was rather minor recession on the other sections. This observation suggests a contact of a large size particle of hard mineral contaminant with the cutting edge not a long time before the end of the test. The HMC particles that might contribute damages of cutting edges no. 1, 2, and 3 can be seen in Fig. 8. Small clearance surface recession suggests that the HTTR have probably have a very small contribution in the total cutting edge wearing process, according to the low value of the R_{MW} quantifier (Table 2). On the worn-out clearance surface of the tool no. 4 after cutting the wood of the *Zelkova serrata* a uniform wear, without scratches in parallel to the cutting speed can be seen (Fig. 16). This observation suggests that iron binder was not abraded by particles of hard mineral contaminants. Randomly distributed, rounded WC carbide grains, visible on the worn surface of the cutting edge, suggests that the HTTR transformed the Fe binder into products that were easily removable by friction. The largest cutting edge recession in case of tool no. 4 was in agreement with the highest value of the R_{MW} quantifier (Table 2).

For the two worn cutting edges nos. 2 and 4, the clearance face recession VB_F was dominant, which might be connected to a large HTTR (no. 4) and content of HMC (no. 2). In these two cases, the recession measured in terms of the bisector of sharpness angle VB_W was also larger than the rake face recession VB_S . For two worn cutting edges nos. 1 and 3, the clearance face recession VB_F was a little lower than in the cases of VB_W and VB_S . In these two cases, the recession measured in the rake face VB_S was dominant.

On the SEM image, Fig. 17, of the *Shorea faguetiana* F., small particles looking like mineral contamination can be seen attached to walls of some cells. There are only single small particles, attached to walls of some cells of the *Japanese Douglas Fir* (Fig. 18). Because of small structures visible on the SEM image of Fig. 19, showing the *Koompassia malaccensis* M.&B. wood, it was very different in comparison to all other SEM images of wood samples. However, no small particles attached to cells walls can be seen in this case.

The SEM image of the *Zelkova serrata* wood (Fig.20) was also very different in comparison to all other SEM wood images, because of large structures having the appearance of bubbles, probably filled up with natural resin. This might be associated with large HTTR and cutting edge wear, similarly to previous observations related to the wood of Keyrung (*Combretocarpus* sp.) (Porankiewicz et al. 2005).

However, for wood specimen no. 1, of the *Shorea faguetiana* F., the case of the lowest content of the HMC, the smallest cutting edge recession was observed for wood specimen no. 2, corresponding to *Japanese Douglas Fir*. Though this was the case with the largest content of the HMC, the highest cutting edge recession was not observed, showing that the cutting edge recession and the content of HMC did not follow each other in all of the experiments considered.

The wood specimen's density D differed from 522 to 880 kg/m³ (Table 1), but the cutting edge recession and the wood density did not follow each other. For wood specimen no. 3, of the *Koompassia malaccensis* M.&B., the case of the largest wood density, the largest cutting edge recession was not observed. Also for wood specimen no. 2, of the *Japanese Douglas Fir*, the case of the smallest wood density, the lowest cutting

edge recession was not observed. These findings suggest that the role of wood density in cutting edge wearing was not large relative to other factors.

An attempt at multi-parameter analysis was performed in order to separate the influence of content C_{MC} and size S_{MC} of the HMC, wood density D , and the HTTR on the cutting edge recession VB_F , as well as verifying the method of evaluation of the HTTR quantifier R_{MW} . For analysis, an algorithm based on modified theoretical simulation method developed in works by Porankiewicz (1993, 2004) was employed.

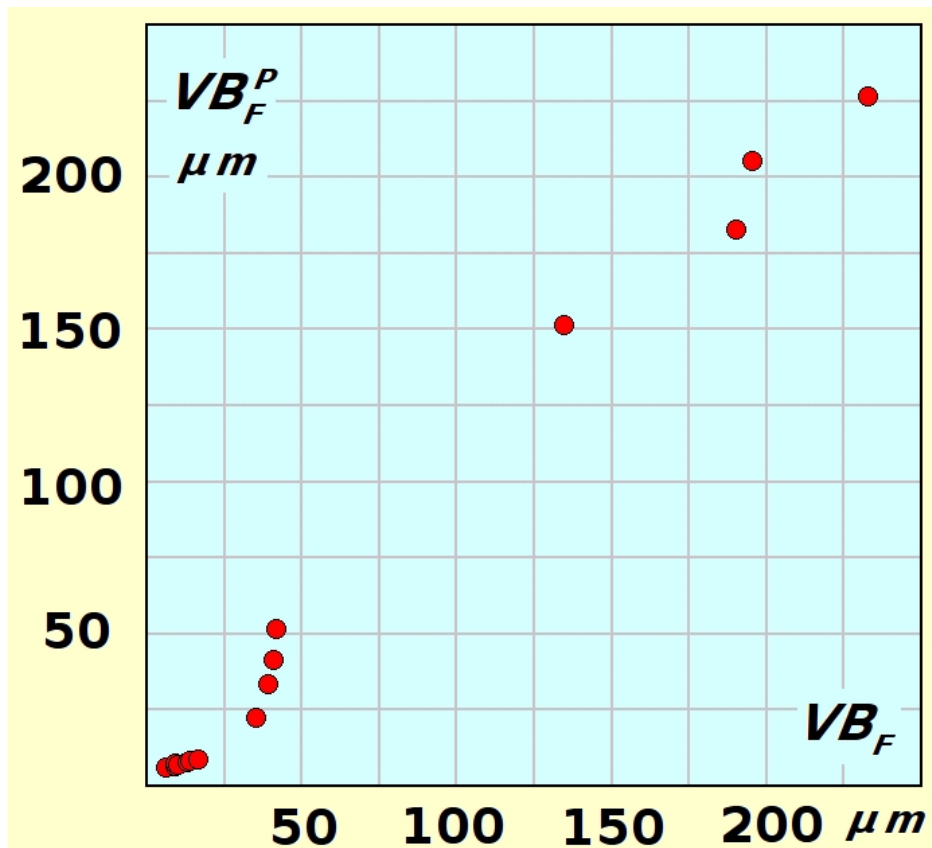


Fig. 21. Plot of observed VB_F cutting edge recession, versus predicted one obtained from theoretical simulation, for method II of evaluation of the R_{MW} quantifier (Fig. 3)

The best approximation was obtained in the case of method II (Fig. 21), as indicated by the lowest summation of square of residuals SK , as high as $SK = 761$, by correlation coefficient as high as $R = 0.99$ between predicted recession VB_F^P , and the recession observed VB_F . For method III, a little higher SK , as high as $SK = 771.4$, was obtained. For method I, a much larger SK , as high as $SK = 1771$, was obtained.

Results from calculations, for method II of R_{MW} quantifier evaluation, also showed that for wood specimen no. 4, of the *Zelkova serrata*, a contribution of the HTTR and the content of HMC particles and the wood density in the total cutting edge recession were as high as 96 %, 51 %, and 1 %, respectively. In this case, a synergistic effect of the HTTR and HMC took place, as large as 43 %. The HTTR appeared to be the most important factor influencing the HSS cutting edge wearing in the case of wood specimen no. 4. For wood specimen no. 2, of the *Japanese Douglas Fir*, the contribution of the

content of HMC particles in the total cutting edge recession reached 85 %. For wood specimen no. 3, of the *Koompassia malaccensis* M.&B., an influence of the HTTR and the content of HMC particles and wood density D in the total cutting edge recession reached 31 %, 5 %, and 2 % respectively. Results of calculations showed that the role of analyzed independent variables was different for the examined wood specimens.

CONCLUSIONS

1. Results of analysis show that the role of analyzed independent variables of the high-temperature tribochemical reactions (HTTR), the mineral contamination, and the wood density was different for each of the examined wood specimens.
2. The HTTR was a main source of large cutting edge recession VB_F in case of the *Zelkova serrata* wood specimen.
3. In the case of wood specimen no. 4, of the *Zelkova serrata*, a significant 43 % synergistic effect of mechanical (caused by the HMC) and chemical (caused by the HTTR) cutting edge wear (recession) was evidenced.
4. The HTTR, expressed by the R_{MW} quantifier calculated according to method II, seems to be the most appropriate for the present type of analysis.
5. Under the cutting conditions applied to wood specimens nos. 4 and 2, the cutting edge recession on the clearance surface VB_F was dominant.
6. For the case of wood specimens nos. 4 and 2, having low HTTR and HMC, the rake face cutting edge recession VB_S was dominant.
7. The dependence of the cutting edge recessions upon the cutting path L_C , $VB = f(L_C)$ was very well described by use of a simple power-type function.
8. According to theoretical simulation performed, the role of the wood density D on the cutting edge recession was very low.

ACKNOWLEDGMENTS

The authors are grateful for the support of the Poznań Networking & Supercomputing Center (PCSS) calculation grant.

REFERENCES CITED

- Amos, G., L. (1952). *Silica in Timbers*. CSIRO, Australia, No. 267.
- Porankiewicz, B. (1993). "Catastrophic wear mechanism when milling particle board," *Proc 11th International Wood Machining Seminar*, Oslo, Norway, 509-514.
- Porankiewicz, B. (2003a). "A method to evaluate the chemical properties of particle board to anticipate and minimize cutting tool wear," *Wood Science & Technology* 37, 47-58.
- Porankiewicz, B. (2003b). "Tępienie się ostrzy i jakość przedmiotu obrabianego w skrawaniu płyt wiórowych" ("Cutting edge wearing and machining quality by particle

board milling"). Printing House, Agricultural University of Poznań, No. 341 (in Polish).

- Porankiewicz, B. (2006). "Theoretical simulation of cutting edge wearing when secondary wood products cutting," *Wood Science & Technology* 40, 107–117.
- Porankiewicz, B., Sandak, J., and Tanaka, C. (2005). "Factors influencing steel tool wear when milling wood," *Wood Science & Technology* 39(3), 225-234.
- Porankiewicz, B., Iskra P., Sandak J., Tanaka, C., and Józwiak, K. (2006). "High speed steel tool wear after wood cutting in presence of high temperature and mineral contamination," *Wood Science & Technology* Vol. 40, 673–682.

Article submitted: April 15, 2008; Peer-review completed: July 9, 2008; Revised version received: July 10, 2008; Accepted and published: July 12, 2008.